JAERI-M
9783

IMPURITY SCREENING OF SCRAPE-OFF PLASMA IN A TOKAMAK

November 1981

Hiroshi KISHIMOTO, Keiji TANI and Hiroo NAKAMURA

日 本 原 子 力 研 究 所
Japan Atomic Energy Research Institute

JAERI-M 9783

Impurity Screening of Scrape-Off Plasma in a Tokamak

Hiroshi KISHIMOTO, Keiji TANI and Hiroo NAKAMURA

Division of Large Tokamak Development,

Tokai Research Establishment, JAERI

(Received October 15, 1981)

Impurity screening effect of a scrape-off layer has been studied in a tokamak, based on a simple model of wall-released impurity behavior. Wall-sputtered impurities are stopped effectively by the scrape-off plasma for a medium-Z or high-Z wall system while major part of impurities enters the main plasma in a low-Z wall system. The screening becomes inefficient with increase of scrape-off plasma temperature. Successive multiplication of recycling impurities in the scrape-off layer is large for a high-Z wall and is enhanced by a rise of scrape-off plasma temperature. The stability of plasma-wall interaction is determined by a multiplication factor of recycling impurities.

Keywords; Tokamak, Plasma-wall Interaction, Impurity Control, Low-Z Wall, Sputtering, Scrape-off Plasma

JAERI－M 9783

トカマクにおけるスクレプオフ層プラズマの不純物遮蔽

日本原子力研究所東海研究所大型トカマク開発部
岸本　浩・谷　啓二・中村博雄

（1981年10月15日受理）

壁面から発する不純物の挙動に関する簡単なモデルに基づいて、トカマクプラズマにおけるスクレプオフ層の不純物遮蔽効果を調べた。高Zないしは中間Z値の壁材をもつ系では、壁でスパッタされた不純物は効果的にスクレプオフ層プラズマでさえぎられるが、低Z値壁の場合は、大部分の不純物が主プラズマ中に進入する。遮蔽効果はスクレプオフ層プラズマの温度の上昇とともに減少する。スクレプオフ層中の再循環不純物の逐次増倍は、高Z値壁について大きく、スクレプオフ層プラズマの温度の増加によってさらに促進される。プラズマー壁相互作用の安定度は、これら再循環不純物の増倍係数によって定まる。

Contents

目　次

1. INTRODUCTION

It is noted well that impurity control is one of the most important problems in tokamak research. Impurity control in a tokamak can be classified typically into two groups, i.e., light impurity control and wall material impurity control. Most of light impurities come from the wall surface on which gaseous impurities such as carbon, nitrogen and oxygen are adsorbed and absorbed. These kinds of impurities can be reduced less than acceptable limits by providing appropriate treatments and conditionings of the wall surface before and after assembly. Control of wall material impurity is in essential difficulty still now and becomes more important in large tokamaks such as JT-60 to achieve a reactor-grade plasma and maintain it during a long discharge.

Several mechanisms were observed as the origion of wall material impurities in actual tokamaks. They were evaporation, arcing and sputtering. Evaporation was induced by a large heat deposition on the wall surface and could be excluded by spreading the heat flux. Arcing was serious in a dirty, unstable discharge and in an early stage of plasma formation. In the steady-state of discharge, sputtering by neutral particles, plasma ions and impurity ions became the dominant process of wall material impurity generation.

It has been demonstrated in divertor experiments that the main plasma of a tokamak discharge is partially screened against wall-released or injected impurities [1]. There is experimental evidence that impurity screening still exists even in a material limiter system. This screening is particularly important in impurity evolution of a tokamak. However little is known about it, and further investigations of this subject are required experimentally and theoretically.

In this paper the impurity screening of a scrape-off plasma is

investigated in a tokamak, based on a simple model of wall-released impurity behavior. Basic analysis of screening effect is described in Section 2. Impurity screening and behavior of a large tokamak are investigated for typical kinds of wall materials such as carbon, titanium and molybdenum. These results are given in Section 3. Impurity evolution of a tokamak plasma is estimated in Section 4 by taking into account of impurity screening effect. Conclusions of the present investigations are summarized in Section 5.

2. SCREENING OF WALL-RELEASED IMPURITIES

The tokamak first wall usually consists of a liner wall and limiters or neutralizer plates. The liner wall is bombarded mainly by neutral particles. The limiters or the neutralizer plates are in contact with the scrape off plasma and are hitted by charged particles. The first wall emits wall material impurities due to sputtering by these incident particles.

The energy and angular distribution of sputtered atoms was derived as following, based on a simple cascade theory [2],

$$\psi(\varepsilon,\theta) = \frac{S}{\pi A} \frac{1-\{(U+\varepsilon)/\Lambda E\}^{1/2}}{\varepsilon^2(1+U/\varepsilon)^3} \cos\theta \quad , \tag{1}$$

where S is the sputtering yield, $(\pi-\theta)$ is the angle between the directions of incident particles and sputtered atoms, E is the incident particle energy, U is the dissociation energy of the wall material, ε is the energy of sputtered atoms, and $\Lambda = 4M_1M_2/(M_1+M_2)^2$ with the incident particle mass M_1 and the sputtered atom mass M_2. From Eq.(1) the sputtered atoms have the maximum energy $\varepsilon_{max} = \Lambda E - U$. The factor A is determined so that

$$\frac{1}{S}\int_0^{\varepsilon_{max}}\int_{-\pi/2}^{\pi/2} \psi \, d\theta \, d\varepsilon = 1 \quad .$$

The sputtered impurity atoms can be ionized and be trapped in the scrape-off layer plasma. The shielding factor λ is then defined by the fraction of trapped atoms among the sputtered atoms. The sputtered atoms without ionization may enter the main plasma or the wall surface. The untrapping factor ξ is determined as the fraction of impurities entering the main plasma. The residual fraction of untrapped impurities

is treated here as to be captured on the wall surface without reemission of wall material atoms.

Emission of wall material atoms is illustrated in Fig.1(a) in case where neutral particles hit the liner wall. Then the untrapping factor is equal to $(1-\lambda)$ and is given by

$$\xi = \frac{1}{S}\int_0^{\varepsilon_{max}} \int_0^{\theta_s} \psi \, d\varepsilon \, d\theta$$

$$= \frac{1}{A}\left\{\frac{1}{\Lambda E}\left(1 - \frac{U+E_s}{6\Lambda E}\right) + \frac{1}{U+E_s}\left(\frac{1}{2}+\frac{2}{3}\frac{E_s}{\sqrt{\Lambda E}\,\sqrt{U+E_s}}\right)\right.$$

$$\left. - \frac{2}{\sqrt{\Lambda E}\,\sqrt{U+E_s}}\left(1-\frac{1}{3}\frac{U}{U+E_s}\right)\right\} \quad , \qquad (2)$$

where $E_s = M_2 d_s^2/2\tau_i^2$ and $\theta_s = \sin^{-1}\sqrt{E_s/\varepsilon}$. The ionization relaxiation time is given by $\tau_i = 1/\overline{n_{es}}\, S_I$, where S_I is the ionization coefficient of neutral impurity atoms to the first charge state [3-5]. Both d_s and $\overline{n_{es}}$ are the scrape-off plasma parameters; scrape-off layer width and average electron density of scrape-off plasma. We can see that E_s means the energy of impurity atoms with the ionization mean free path equal to the scrape-off layer width.

The shielding factor λ for neutral particle bombardment is given in Fig.2 as a function of incident energy E. It appears that λ becomes small with increase of E and that λ becomes large as E_s is increased.

The feature of impurity screening is shown in Fig.1(b) for charged particles interacting with limiters or neutralizer plates. The shielding factor for these charged particles is given by

$$\lambda = \frac{1}{S}\int_0^{\varepsilon_{max}} \int_{\Omega(\varepsilon)} \psi \, d\varepsilon \, d\omega$$

$$= \frac{4}{\pi A}\int_0^{\varepsilon_{max}} \frac{1-\{(U+\varepsilon)/\Lambda E\}^{1/2}}{\varepsilon^2(1+U/\varepsilon)^3} d\varepsilon \int_{-1/2}^{1/2} (1-\frac{E_s}{\varepsilon}x)^{1/2} dx$$

$$= 1-\frac{2}{A}\int_{E_s/4}^{\varepsilon_{max}} \frac{\varepsilon}{(\varepsilon+U)^3}\{1-(\frac{\varepsilon+U}{\Lambda})^{1/2}\}(\frac{1}{2}-\frac{\theta_s'}{\pi}-\frac{\sin 2\theta_s'}{2\pi})d\varepsilon \ , \quad (3)$$

where $\Omega(\varepsilon)$ is the solid angle of a semi-sphere with radius $d_s(\varepsilon/E_s)^{1/2}$ bounded by the scrape-off layer at $(-d_s/2, +d_s/2)$ and $\theta_s' = \sin^{-1}\sqrt{E_s/4\varepsilon}$. For material limiters we can take the untrapping factor as $\xi = (1-\lambda)/2$. The residual half of sputtered atoms is attached to the wall surface. In an ideal divertor it can be assumed that $\xi = 0$, which means that unshielded impurities are captured completely by the divertor chamber wall.

Finally in this section the behavior of shielded impurities must be considered. These impurities will undergo recycling in the scrape-off layer as investigated numerically in Ref.[6] by Monte Carlo techniques. This process will be analysed here in a more simple way.

The trapped impurities move along the magnetic field lines in the scrape-off layer with the initial velocity related to the averaged sputtered energy

$$\bar{\varepsilon} = \int \varepsilon \, \psi \, d\varepsilon \Big/ \int \psi \, d\varepsilon \quad .$$

After relaxiation of the initial velocity by collision, the impurities are swept out toward the nearest neighbor limiter or neutralizer plate with the velocity equal to the scrape-off plasma flow velocity v_f. In accordance with these traveling motions impurities experience successive ionization by electron impact. These impurities reenter the limiter

(neutralizer plate) after accelerated by the sheath potential and emit the next generation impurities. The charge state of impurities until relaxiation can be given by

$$\sum_{j=1}^{Z_r} \frac{\tau_i^{j+1}}{\tau_r^{j}} = 1 \quad ,$$

where τ_r^{j} is the velocity relaxiation time of impurities with the j-th charge state and $\tau_i^{j+1} = 1/\overline{n_{eb}} S_{j+1}$ is the ionization relaxiation time of impurities from the j-th state to the (j+1)-th state. The average charge state of reentering impurities $\bar{Z}$ is given by

$$\sum_{j=1}^{Z_r} \tau_i^{j+1} + \frac{\ell_r}{v_f} = \sum_{j=1}^{\bar{Z}} \tau_i^{j+1} \quad , \tag{4}$$

where ℓ_r is the distance between the velocity relaxiation point of sputtered atoms and the nearest neighbor limiter. We should note that the pre-sheath potential of the scrape-off plasma [7] is neglected here for simplicity.

The above-mentioned process continues successively and the impurity content in the scrape-off layer reaches a saturation or grows up unstably. During this recycling process the inward flow of impurities may occur from the scrape-off layer to the main plasma. We will denote by η the inward flow fraction of impurities in one cycle. Then the effective untrapping factor can be represented by

$$\xi_{eff} = \xi + \lambda\{\eta + \xi_R S_R (1-\eta)\} \sum_{k=0}^{\infty} \{(1-\eta)\lambda_R S_R\}^k \tag{5}$$

for material limiter system and

$$\xi_{eff} = \xi + \lambda\eta \sum_{k=0}^{\infty} \{(1-\eta)\lambda_R S_R\}^k \qquad (6)$$

for ideal divertor system with $\xi_R = 0$. In Eqs.(5) and (6) ξ_R, λ_R and S_R are the untrapping factor, the shielding factor and the self-sputtering yield of the recycling impurities, respectively. It can be seen from Eqs.(5) and (6) that the stability of the impurity recycling process is determined by the impurity multiplication factor $(1-\eta)\lambda_R S_R$: the recycling process is stable for $(1-\eta)\lambda_R S_R < 1$ and the plasma-wall interaction system has no equilibrium state for $(1-\eta)\lambda_R S_R \geq 1$.

3. IMPURITY BEHAVIOR IN SCRAPE-OFF LAYER

3.1 Scrape-off Plasma Parameters

The main plasma of a tokamak discharge is separated from the material wall by a scrape-off layer plasma. The scrape-off plasma is in contact with the limiters or the neutralizer plates of divertor at its ends. The scheme of the plasma and first wall is illustrated in Fig.4. The length along the field line of the scrape-off plasma is taken as $L = L_1 + 2L_2$, where L_1 is the field line length of the main plasma surface and L_2 is that of the divertor chamber. The diffusion coefficient $D_\perp$ and the flow velocity v_f of the scrape-off plasma are taken from the empirical scalings of DIVA [8]: $D_\perp = 0.5 D_B$ and $v_f = 0.3 c_s$ where D_B is the Bohm diffusion coefficient and c_s is the ion sound velocity. The thickness of the scrape-off layer is given by $d_s = \sqrt{\tau_{//} D_\perp}$ where $\tau_{//} = L/v_f$. The scrape-off plasma density is obtained from particle conservation as

$$\overline{n_{es}} = \frac{1}{2} \frac{a}{d_s} \frac{\tau_{//}}{\tau_p} \frac{L_1}{L} \bar{n}_e \quad . \tag{7}$$

Here a, τ_p and $\bar{n}_e$ are the minor radius, the particle confinement time and the average density of the main plasma, respectively. If the particle confinement time is predicted by the Alcator-like scaling; $\tau_p = 3 \times 10^{-21} \sqrt{q_a}\, \bar{n}_e\, a^2$ in MKS units, Eq.(7) becomes that

$$\overline{n_{es}} = \frac{10^{21}}{6} \frac{\tau_{//}}{d_s\, a \sqrt{q_a}} \frac{L_1}{L} \quad . \tag{8}$$

Parameters used in the present paper are as following: major radius R = 3 m, a = 1 m, $q_a = 3$, toroidal field $B_T = 5$ T, L = 42 m with $L_1 = 30$ m in divertor system, L = 10 m in material limiter system, and plasma species

are hydrogens.

3.2 Sheath Potential

A sheath potential ϕ is formed in front of the limiters or the neutralizer plates and influences significantly the impurity behavior of a scrape-off plasma. The incident energy of ions onto the limiters is given by

$$E = E_0 + Z e \phi \quad , \tag{9}$$

where E_0 is the average energy of ions on the sheath boundary and Z is the ion charge. The sheath potential was derived by Hobbs and Wesson [9] as

$$e\phi = k T_{eb} \ell n \frac{1-\gamma_e}{\sqrt{2\pi m/M}} \quad , \tag{10}$$

where γ_e is the secondary electron emission coefficient for thermal electron incidence, m/M is the mass ratio of electron to plasma ion, and T_{eb} is the electron temperature of the scrape-off plasma. The sheath stability criterion requires that $E_0 \gtrsim kT_{eb}/2$. When γ_e increases toward unity, the sheath potential is saturated at

$$e\phi = 1.02\ kT_{eb} \tag{11}$$

for $\gamma_e \gtrsim 0.8$.

The sheath potential for typical wall materials such as carbon, titanium and molybdenum is shown in Fig.5 as function of scrape-off plasma temperature T_{eb}. Here an enhancement of γ_e due to oblique incidence is taken into account by a factor 1.5 and the values of γ_e for the thermal electron incidence are obtained by folding γ_e of monoenergetic electron

incidence with a maxwellian distribution function. It can be seen in Fig.5 that the sheath potential saturates at 1.02 T_{eb} in the temperature range of 100 eV $\lesssim T_{eb} \lesssim$ 1000 eV because γ_e becomes large over 0.8. For sufficiently small γ_e the sheath potential varies proportionally with T_{eb} as $e\phi = kT_{eb}\ \ell n\sqrt{M/2\pi m}$.

3.3 Shielding Factor and Untrapping Factor

Charge-exchange neutrals are emitted from the main plasma and hit the liner wall. The outflux and energy spectrum of these neutral atoms can be calcurated by an one-dimensional integral equation code [10]. The sputtered flux of wall material y_{cx} is given by

$$y_{cx} = \int_0^\infty S_H \Gamma_{cx} f_{cx}(E) dE \qquad (12)$$

where S_H is the sputtering yield due to hydrogen bombardment, Γ_{cx} is the outflux of charge-exchange neutrals and $f_{cx}(E)$ is the energy distribution function of charge-exchange neutrals. Providing that the radial distributions of density and temperature of the main plasma are represented by

$$n_e(r) = n_{e0} \{1 - (r/a)^4\}$$

$$T_e(r) = T_i(r) = T_0 \{1 - (r/a)^2\} \quad ,$$

the sputtered impurity flux y_{cx} is estimated as shown in Fig.6 in case of molybdenum wall. It can be seen that y_{cx} increases with the average temperature $\bar{T}_e$ and becomes small with increase of the average electron density $\bar{n}_e$. The averaged untrapping factor $\bar{\xi}_{cx}$ or shielding factor $\bar{\lambda}_{cx}$ is given by

$$\bar{\xi}_{cx} = 1 - \bar{\lambda}_{cx} = \int_0^\infty \xi_{cx}(E) f_{cx}(E) dE \Big/ \int_0^\infty f_{cx}(E) dE \quad , \qquad (13)$$

where ξ_{cx} is the untrapping factor associated with the monoenergetic neutral particle incidence. The average untrapping factor is shown in Fig.7 as function of scrape-off plasma temperature for three kinds of wall materials; carbon, titanium and molybdenum. It turns out that the carbon wall exhibits large values of $\bar{\xi}_{cx}$ either with material limiter or with divertor. The untrapping impurity fraction decreased with the mass number of wall material. Divertor is quite effective for shielding the high-z wall impurities due to the increased scrape-off layer width and plasma density. It is noteworthy that the impurity shielding effect becomes inefficient significantly as the scrape-off plasma temperature increases.

Charged particles such as plasma ions and impurity ions diffuse from the main plasma into the scrape-off layer and enter the limiter surface after accelerated by the sheath field. The shielding factor against these charged particles are shown in Fig.8 in case of material limiter system. The charge state of impurity ions are estimated from a coronal equilibrium model. The situations are similar to those of neutral particle incidence. The shielding effect is less significant for self-sputtering than for plasma ion sputtering. In a divertor system impurities emitted from the neutralizer plates are shielded more than in the material limiter system.

The effective untrapping factor ξ_{eff} can be estimated from Eqs.(5) and (6). Then we need the values of ξ_R, S_R and η. The untrapping factor of recycling impurities is obtained by analysing the impurity ion motion in cooporation with the electron impact ionization process as described in Section 3. Concerning the sputtering yield of recycling impurities S_R, we have little of experimental data for the self-sputtering yield S_z. Thereby we have employed an empirical scaling [11]

$$\frac{S_z}{M_z} = 6.4 \times 10^{-3} A^{5/3} E'^{1/4} \left(1 - \frac{1}{E'}\right)^{7/2} \qquad (14)$$

for the incident energy range of $E' \lesssim 20$ and extraporated it beyond the energy $E' \sim 20$ so as to fit the experimental data obtained at $E = 45$ keV [12], where $E' = E/E_{th}$ with the incident energy E and the threshhold energy E_{th}. The self-sputtering yields of carbon, titanium and molybdenum are shown in Fig.9 as function of incident energy of impurity ions. The evaluations of the inward flow fraction of impurity ions from the scrape-off layer into the main plasma is a difficult problem still now and further investigations on this subject are required. An experiment on divertor suggested that the inward flow of impurities might be small [1]. Hence we have introduced the neoclassical transport theory [13] for η.

The relation of average charge state $\bar{z}$ of recycling impurities versus scrape-off plasma temperature T_{eb} is shown in Fig.10 in case of material limiter. The average charge state increases as the scrape-off plasma temperature is risen. At sufficiently high temperature of scrape-off plasma the sputtered atom velocity becomes high due to the incident energy increase by the sheath-acceleration of impurity ions and thereby the recycling impurities reach limiters or neutralizer plates before they experience sufficient electron-impact ionization. The impurity multiplication factor $\lambda_R S_R(1-\eta)$ is shown in Fig.11 against the scrape-off plasma temperature in the material limiter system. The first wall made of carbon or titanium has a stable nature of impurity recycling process because $\lambda_R S_R(1-\eta) < 1$ is obtained at any value of T_{eb}. In the meanwhile the molybdenum limiter system has no equilibrium state at T_{eb} larger than about 50 eV. Because of the employment of the neoclassical inward transport the contribution of inward flux of impurities is not significant in these estimations.

4. IMPURITY EVOLUTION IN MAIN PLASMA

The simple model of impurity behavior developed in Section 2 seems to be suitable to be included in an one dimensional tokamak transport code. In stead of this we will consider here the impurity evolution problem based on the zero dimensional particle balance equation described by

$$\frac{d\bar{n}_z}{dt} = -\frac{\bar{n}_z}{\tau_z} + (\xi_H S_H \frac{\bar{n}_e}{\tau_p} + \xi_z S_z \frac{\bar{n}_z}{\tau_z}) + \frac{A_w}{V_p} \xi_{cx} y_{cx} \quad , \tag{15}$$

where $\bar{n}_z$ is the average density of impurity ions in the main plasma, τ_z is the confinement time of impurity ions, ξ is the effective untrapping factor, S is the sputtering yield, y_{cx} is the sputtered impurity flux due to charge-exchange neutral bombardment, A_w is the surface area of the liner wall, and V_p is the plasma volume. Suffixes H, z and cx indicate the incidences of plasma ions, wall material impurity ions and charge-exchange neutrals, respectively. Equation (15) can be solved as

$$\bar{n}_z(t) = T_z(\xi_H S_H \frac{\bar{n}_e}{\tau_p} + \frac{A_w}{V_p} \xi_{cx} y_{cx})(1 - e^{-(t-t_0)/T_z}) + \bar{n}_z(t_0)\, e^{-(t-t_0)/T_z} \quad , \tag{16}$$

where $\bar{n}_z(t_0)$ is the impurity ion density at a time t_0. The time constant of impurity evolution T_z is represented by

$$T_z = \frac{\tau_z}{1 - \xi_z S_z} \quad . \tag{17}$$

The impurity evolution time becomes large as $\xi_z S_z$ increases toward unity. The impurity cencentration of the main plasma $\alpha = \bar{n}_z/\bar{n}_e$ approaches the

following saturation level with the time development:

$$\alpha_s = \left(\frac{\xi_H S_H}{\tau_p} + \frac{A_w}{V_p}\frac{\xi_{cx} y_{cx}}{\bar{n}_e}\right) T_z \qquad (18)$$

Providing that $\tau_z = \tau_p$ and that the limiters and the liner walls are made of the same material, the saturated impurity content α_s is estimated as function of the scrape-off plasma temperature T_{eb} in the material limiter system. The relation of α_s versus T_{eb} is shown in Fig.12. The impurity concentration of the carbon wall or the titanium one shows a stable behavior against the change of T_{eb}. In the meanwhile the molybdenum wall system exhibits an unstable feature of the impurity concentration with the scrape-off plasma temperature larger than about 50 eV. These behaviors of impurity concentration are surely caused from the impurity shielding effect of the scrape-off layer and from the impurity multiplication process in the scrape-off layer.

5. CONCLUSIONS

Impurity screening effect of a scrape-off layer has been analysed, based on a simple model of wall-released impurity behavior. Following conclusions are obtained in the present investigation.

(a) Impurity screening of a scrape-off layer is more effective in the medium-Z or high-Z wall system rather than in the low-Z wall system.

(b) Impurity screening becomes inefficient with the increase of the scrape-off plasma temperature.

(c) Multiplication process of recycling impurities in a scrape-off layer plays an important role in the impurity evolution of the main plasma. The key parameter for this process is $\lambda_R S_R(1-\eta)$ with the shielding factor λ_R, the sputtering yield S_R and the impurity inward flow fraction η of the recycling impurities.

In a reactor-grade tokamak suprathermal particles such as beam ions associated with neutral beam injection and alpha particles due to D-T reaction influence the impurity generation. This kind of problem was treated in Ref.[14]. Further investigation concerning the impurity behavior in a scrape-off layer may be required for the following subjects; pre-sheath electric field formed in a scrape-off layer, impurity ion transport process between the main plasma and the scrape-off plasma, and the effect of plasma particle accumulation in a divortor chamber on the impurity behavior of a scrape-off layer.

ACKNOWLEDGEMENT

The autors are grateful to Drs. A. Tomabechi, M. Yoshikawa, T. Hiraoka and T. Iijima for their support and encouragement during this work.

5. CONCLUSIONS

Impurity screening effect of a scrape-off layer has been analysed, based on a simple model of wall-released impurity behavior. Following conclusions are obtained in the present investigation.

(a) Impurity screening of a scrape-off layer is more effective in the medium-Z or high-Z wall system rather than in the low-Z wall system.

(b) Impurity screening becomes inefficient with the increase of the scrape-off plasma temperature.

(c) Multiplication process of recycling impurities in a scrape-off layer plays an important role in the impurity evolution of the main plasma. The key parameter for this process is $\lambda_R S_R(1-\eta)$ with the shielding factor λ_R, the sputtering yield S_R and the impurity inward flow fraction η of the recycling impurities.

In a reactor-grade tokamak suprathermal particles such as beam ions associated with neutral beam injection and alpha particles due to D-T reaction influence the impurity generation. This kind of problem was treated in Ref.[14]. Further investigation concerning the impurity behavior in a scrape-off layer may be required for the following subjects; pre-sheath electric field formed in a scrape-off layer, impurity ion transport process between the main plasma and the scrape-off plasma, and the effect of plasma particle accumulation in a divortor chamber on the impurity behavior of a scrape-off layer.

ACKNOWLEDGEMENT

The autors are grateful to Drs. A. Tomabechi, M. Yoshikawa, T. Hiraoka and T. Iijima for their support and encouragement during this work.

REFERENCES

[1] NAGAMI, M., SHIMOMURA, Y., MAEDA, H., KASAI, S., YAMAUCHI, T., SENGOKU, S., SUGIE, T., YAMAMOTO, S., ODAJIMA, K., KIMURA, H., OHASA, K., Nucl. Fusion 18 (1978) 1347.

[2] THOMPSON, M.W., Philos. Mag. 18 (1968) 377.

[3] LOTZ, W., Electron-Impact Ionization Cross-Sections and Ionization Rate Coefficients for Atoms and Ions from Hydrogen to Calcium, IPP 1/62, 1967.

[4] LOTZ, W., Electron-Impact Ionization Cross-Sections and Ionization Rate Coefficients for Atoms and Ions from Scandium to Zinc, IPP 1/76, 1968.

[5] HINNOV, E., On Multiple Ionization in High-Temperature Plasmas, MATT-777, 1970.

[6] SENGOKU, S., AZUMI, M., MATSUMOTO, Y., MAEDA, H., and SHIMOMURA, Y., Nucl. Fusion 19 (1979) 1327.

[7] TAKIZUKA, T., AZUMI, M., SEKI, Y., SENGOKU, S., MAKI, K., SHINYA, K., SUGIHARA, M., YAMAMOTO, S., ODAJIMA, K., KIMURA, H., OHASA, K., NAGAMI, M., SUGIE, T., KASAI, T., MAEDA, H., FUNAHASHI, A., SHIMOMURA, Y., Presented in 8th IAEA Conf. on Plasma Physics and Controlled Nuclear Fusion Research, Brussels, 1980, paper CN-38/x-2-1.

[8] SHIMOMURA, Y. and MAEDA, H., J. Nuclear Materials 76 & 77 (1978) 45.

[9] HOBBS, G.D. and WESSON, J.A., Plasma Physics 9 (1967) 85.

[10] KOBAYASHI, T., TAZIMA, T., TANI, K., TAMURA, S., The Effect of Plasma Minor-radius Expansion in the Current Build-up Phase of a Large Tokamak, JAERI-M 7014, 1977.

[11] ROTH, J., BOHDANSKY, J. and MARTINELLI, A.P., Radiation Effects 48 (1980) 213.

[12] ALMÉN, O. and BRUCE, G., Nuclear Instrum. & Methods 11 (1961) 279.

[13] HIRSHMAN, S.P., Phys. Fluids 19 (1976) 155.

[14] KISHIMOTO, H., TANI, K., and NAKAMURA, H., submitted to Jap. Journal of Appl. Physics.

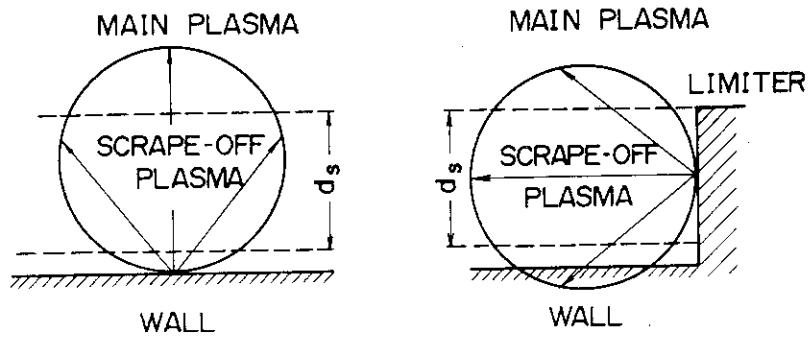

Fig. 1 Schematic of wall-released impurity shielding by scrape-off layer.

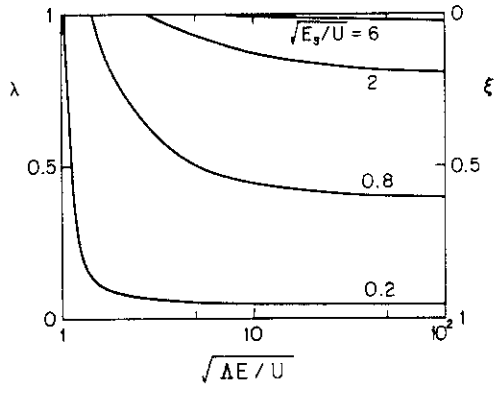

Fig. 2 Relation between impurity shielding factor λ and reduced incident particle energy $\sqrt{\Delta E/U}$ in case of neutral particle incidence onto liner wall.

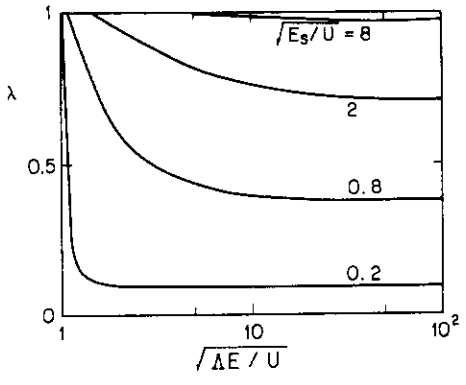

Fig. 3 Relation between impurity shielding factor λ and reduced incident particle energy $\sqrt{\Delta E/U}$ in case of charged particle incidence onto limiter.

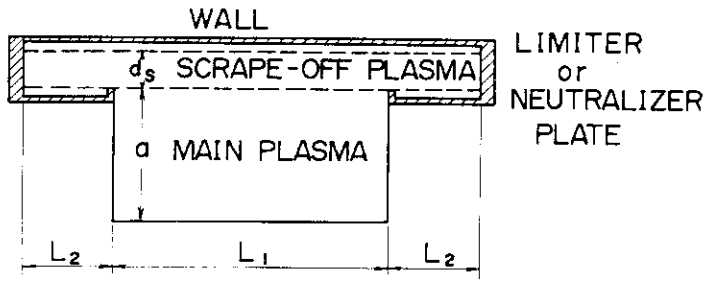

Fig. 4 Schematic model of plasma-wall system.

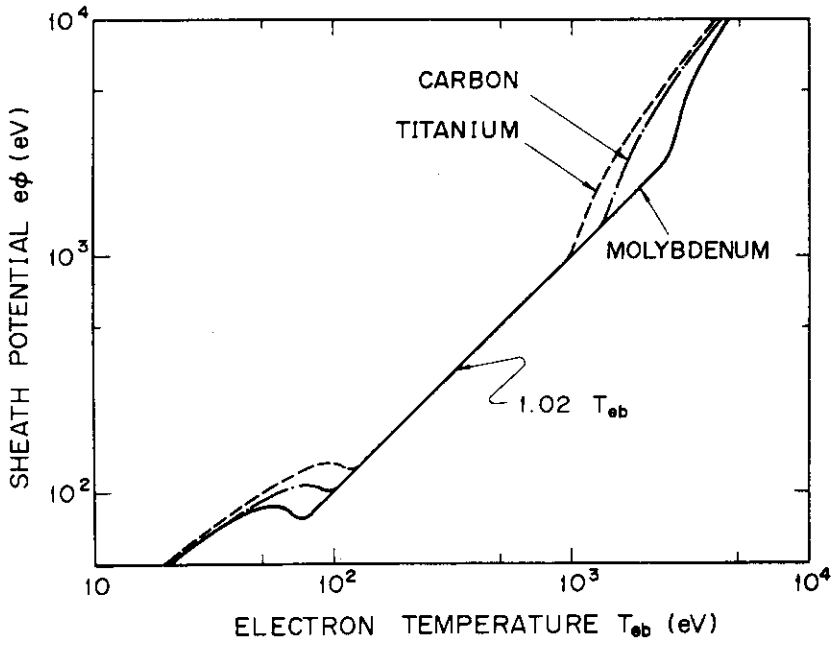

Fig. 5 Relation between sheath potential eϕ and electron temperature of scrape-off plasma T_{eb} for typical limiter materials; carbon, titanium and molybdenum.

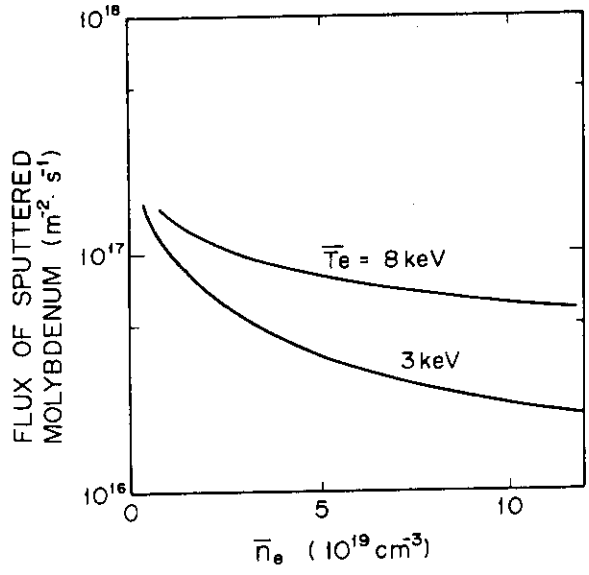

Fig. 6 Sputtered flux of liner wall material atoms due to charge-exchange neutral bombardment in case of molybdenum wall. Parameters of $\bar{n}_e$ and $\bar{T}_e$ are the average electron density and electron temperature of a main plasma.

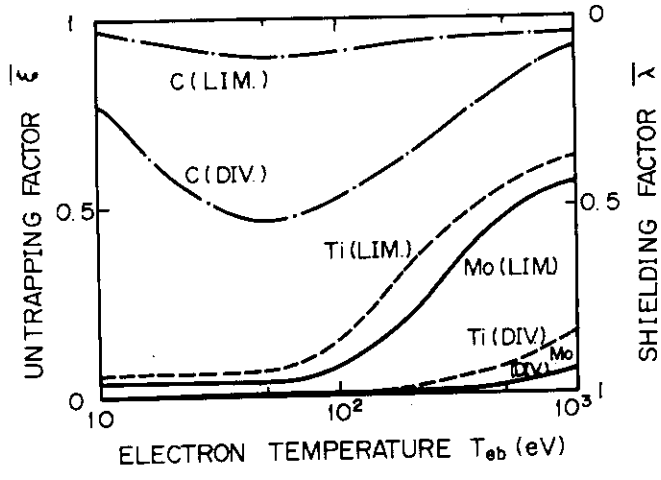

Fig. 7 Untrapping factor ξ of sputtered impurities due to charge-exchange neutrals against scrape-off plasma temperature T_{eb} for bombardment of charge-exchange neutrals emitted from main plasma with $\bar{n}_e = 1\times10^{20}$ m^{-3} and $\bar{T} = 10$ keV. "LIM" indicates material limiter system and "DIV" denotes divertor system.

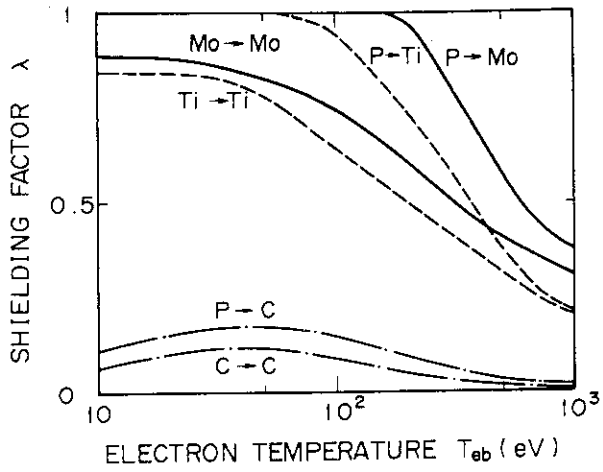

Fig. 8 Impurity shielding factor λ versus scrape-off plasma temperature T_{eb} for proton incidence and material impurity ion incidence.

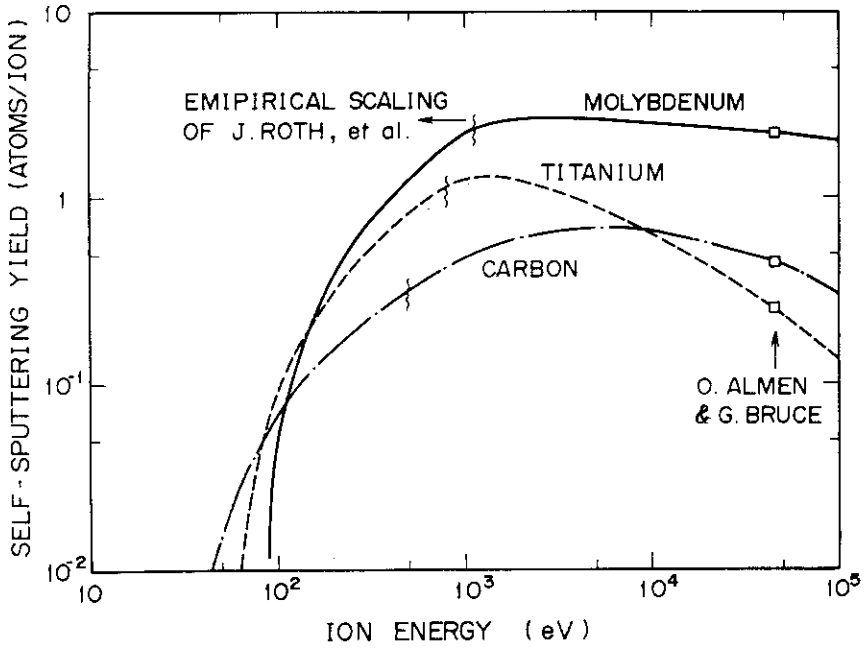

Fig. 9 Self-sputtering yields of carbon, titanium and molybdenum obtained from empirical formula.

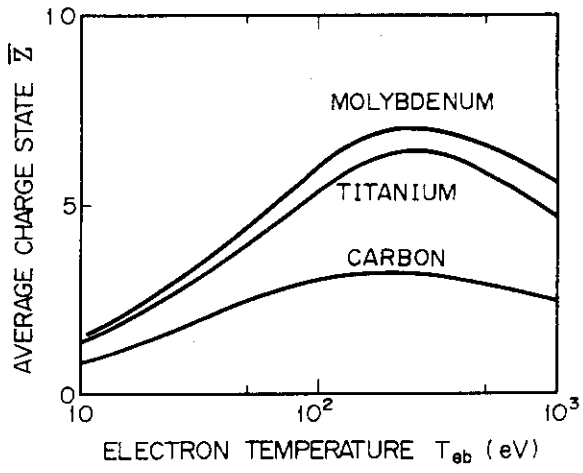

Fig. 10 Average charge state $\bar{Z}$ of recycling impurities versus scrape-off plasma temperature T_{eb} in material limiter system.

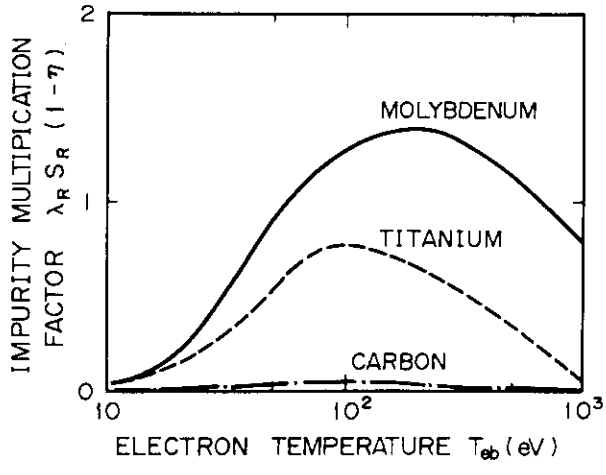

Fig. 11 Multiplication factor of recycling impurities $\lambda_R S_R (1-\eta)$ versus scrape-off plasma temperature T_{eb} with neoclassical inward transport of impurity ions in material limiter system.

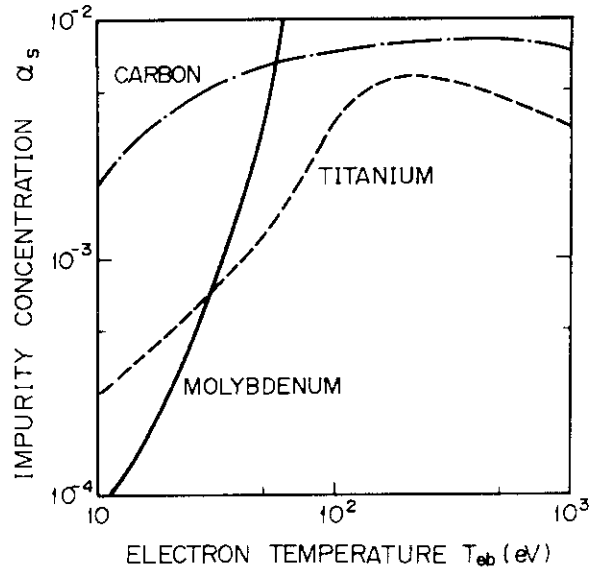

Fig. 12 Impurity evolution of main plasma in material limiter system with $\bar{n}_e = 1\times10^{20}$ m^{-3} and $\bar{T} = 10$ keV.